TIGAR promotes growth, survival and metastasis through oxidation resistance and AKT activation in glioblastoma

ZHI TANG and ZHENGWEN HE

Department of Neurosurgery, Hunan Cancer Hospital and The Affiliated Cancer Hospital of Xiangya School of Medicine, Central South University, Changsha, Hunan 410013, P.R. China

Abstract. Glioblastoma has a poor prognosis and is one of the most lethal types of cancer in the world. TP53 induced glycolysis regulatory phosphatase (TIGAR) is upregulated in various types of cancer. Therefore, the present study investigated the role of TIGAR in glioblastoma. TIGAR expression was measured in glioma samples and cell lines using immunohistochemistry and western blotting. Reduced nicotinamide adenine dinucleotide phosphate (NADPH), glutathione, malondialdehyde and intracellular reactive oxygen species levels were detected to measure oxidative stress in U-87MG cells following short hairpin RNA (shRNA)-mediated knockdown of TIGAR. Cell viability was determined using an MTT assay for TIGAR-overexpression vector- and TIGAR-shRNA-transfected U-87MG cells. Apoptosis was assessed to evaluate whether TIGAR knockdown sensitized cells to the antitumor effects of temozolomide (TMZ). Migration, invasion and epithelial-mesenchymal transition (EMT) were further assessed using Transwell and western blotting assays. A co-immunoprecipitation assay was used to detect the interaction between TIGAR and protein kinase B (AKT). The results of the present study revealed that TIGAR was positively associated with poor survival and was upregulated in glioblastoma. TIGAR knockdown significantly increased oxidative stress, decreased cell proliferation and exacerbated TMZ-induced apoptosis in U-87MG cells. Additionally, TIGAR knockdown decreased migration, invasion and EMT, and treatment of TIGAR-shRNA-transfected cells with NADPH had no effect on metastasis. In addition, TIGAR promoted AKT activation and bound to AKT. In conclusion, the present study demonstrated that TIGAR may promote glioblastoma growth and progression through oxidation resistance and AKT activation.

Introduction

Glioblastoma is the most common type of malignant brain cancer in adults around the world (1). Despite the rapid development of surgical techniques and radiotherapy, and the widespread use of chemotherapy drugs, such as temozolomide (TMZ), glioblastoma continues to be associated with poor prognosis, with a 5-year survival rate of 5-13%, along with a high recurrence rate (2). Therefore, it is important to explore the molecular mechanisms underlying the occurrence and progression of glioblastoma, and to identify novel therapeutic targets to improve glioblastoma treatment and prognosis.

TP53 induced glycolysis regulatory phosphatase (TIGAR) is located on chromosome 12p13.3 and includes six coding exons and two p53 binding sites (3). A previous study has demonstrated that TIGAR is similar to phosphoglucose mutagenesis enzyme and has biphosphatase activity to decompose fructose 2,6-bisphosphate (FB) (4). FB is the allosteric activator of phosphofructose kinase (PFK). Therefore, TIGAR inhibits PFK activity by decreasing FB and directs metabolic flow from glycolysis to the pentose phosphate pathway (PPP) (4). The PPP provides phosphate ribose for nucleic acid synthesis. Reduced nicotinamide adenine dinucleotide phosphate (NADPH), as a byproduct of the PPP, is the main reactive oxygen species (ROS) scavenger in cells. Additionally, TIGAR is overexpressed in several types of cancer, including leukemia (5), lung cancer (6), breast cancer (7), liver cancer (8) and colon cancer (9). TIGAR is considered to protect cancer cells against ROS-induced apoptosis and to induce DNA damage repair (10).

To the best of our knowledge, a role for TIGAR in glioblastoma has not been reported. The present study revealed that TIGAR was overexpressed in glioblastoma and is a potential novel prognostic and migration marker in patients with glioblastoma. Additionally, TIGAR decreased oxidative stress in glioblastoma cells through PPP-mediated NADPH generation. The present study demonstrated that TIGAR knockdown led to significant inhibition of proliferation, migration and invasion in U-87MG cells in an oxidative stress-independent manner. In addition, TIGAR interacted with protein kinase B (AKT) and promoted AKT activation. The results of the present study

Correspondence to: Professor Zhengwen He, Department of Neurosurgery, Hunan Cancer Hospital and The Affiliated Cancer Hospital of Xiangya School of Medicine, Central South University, 283 Tongzipo Road, Changsha, Hunan 410013, P.R. China
E-mail: hezhw2000@163.com

suggested that TIGAR, as an important mediator of glioma progression, may be a potential therapeutic target in glioblastoma.

Materials and methods

Reagents. Bovine serum albumin (BSA), NADPH (cat. no. ST360), dichloro-dihydro-fluorescein diacetate (DCFH-DA; cat. no. S0033-1) and rabbit immunoglobulin G (IgG; cat. no. A7016) were purchased from Beyotime Institute of Biotechnology. Fetal bovine serum (FBS) was purchased from Thermo Fisher Scientific, Inc. Lipofectamine® 2000 reagent was purchased from Invitrogen (Thermo Fisher Scientific, Inc.). The GTVisin™ anti-mouse/anti-rabbit immunohistochemical analysis kit was purchased from Gene Company, Ltd. Anti-TIGAR (cat. no. sc-166290; 1:1,000 dilution), anti-B cell lymphoma 2 (Bcl2; cat. no. sc-509; 1:1,000 dilution), anti-Bcl2-associated X protein (BAX; cat. no. sc-20067; 1:1,000 dilution), anti-α-smooth muscle actin (α-SMA; cat. no. sc-53142; 1:1,000 dilution), anti-E-cadherin (cat. no. sc-71009; 1:1,000 dilution), anti-N-cadherin (cat. no. sc-59987; 1:1,000 dilution), anti-Snail (cat. no. sc-271977; 1:1,000 dilution), anti-Vimentin (cat. no. sc-80975; 1:1,000 dilution) and HRP-conjugated goat anti-mouse IgG (m-IgGκ BP-HRP; cat. no. sc-516102; 1:4,000 dilution) were purchased from Santa Cruz Biotechnology, Inc. Anti-phosphoinositide 3-kinase (PI3K; cat. no. ab191606; 1:1,000 dilution) and anti-phosphorylated (p)-PI3K p85 α (cat. no. ab182651; 1:1,000 dilution) were obtained from Abcam. Anti-AKT (cat. no. 4685; 1:1,000 dilution), anti-p-AKT (Ser473; cat. no. 4060; 1:1,000 dilution), anti-β-Actin (cat. no. 3700; 1:3,000 dilution) and HRP-conjugated goat anti-rabbit IgG (cat. no. 7074; 1:4,000 dilution) antibodies, as well as a mouse IgG control (cat. no. 5415), rabbit IgG control (cat. no. 3900) and radioimmunoprecipitation assay (RIPA) buffer (cat. no. 9806), were purchased from Cell Signaling Technology, Inc. Dimethyl sulfoxide (DMSO), isopropanol, ethanol and chloroform were purchased from Sinopharm Chemical Reagent Co., Ltd.

Cell culture. The human glioblastoma cell lines LN-18, LN-229, U-87MG, U-251MG and SNB-19 were purchased from the Shanghai Institute of Biochemistry and Cell Biology and were authenticated by short tandem repeat profiling. The U-87MG American Type Culture Collection cell line used in the present study is most likely a glioblastoma cell line, but of unknown origin. The cells were cultured in Dulbecco's Modified Eagle's medium (DMEM, Gibco; Thermo Fisher Scientific, Inc.) without any antibiotics, supplemented with 10% FBS (Hangzhou Sijiqing Bio-engineering Material Co.) at 37˚C in a humidified atmosphere with 5% CO_2.

RNA interference and transfection. A total of $2x10^4$ U-87MG cells were infected with 4 μl of $1x10^9$ viral particles of LV-TIGAR-short hairpin RNA (shRNA; 5'-GATTAGCAG CCAGTGTCTTAG-3') or negative control (nc)-shRNA (5'-TTACCGAGACCGTACGTAT-3'), which were synthesized by Shanghai GenePharma Co., Ltd. After 2 days, the transfected cells were selected for using DMEM containing 2 μg/ml puromycin in subsequent experiments.

pcDNA3.1 and pcDNA3.1-TIGAR (human) were purchased from Cyagen Biosciences, Inc. A total of $1.8x10^5$ U-87MG cells in 6-well plates were transfected with 2 μg of either plasmid using 4 μl of Lipofectamine® 2000, and complete medium was added to the cells 6 h after transfection. After further culturing for 36 h, subsequent experiments were performed. For TIGAR dependent AKT activation, $1.8x10^5$ U-87MG cells in 6-well plates were transfected with 1, 2 or 3 μg pcDNA3.1-TIGAR using 4 μl of Lipofectamine® 2000, and complete medium was added to the cells 6 h after transfection. After a further 36 h, cells were lysed, and AKT and p-AKT were detected using western blot assay.

Cell viability. U-87MG/NC cells, U-87MG/sh-TIGAR cells and U-87MG cells transfected with pcDNA3.1 or pcDNA3.1-TIGAR were seeded into a 96-well culture plate at a density of $3x10^4$ cells/well. Cell proliferation was measured at 24, 48, 72 and 96 h. MTT (1 mg/ml dissolved in PBS; 100 μl/well; Sigma-Aldrich; Merck KGaA) was added, and the cells were cultured for 4 h at 37˚C prior to adding 100 μl DMSO. The absorbance was determined using a multiplate reader (SpectraMax 190; Molecular Devices, LLC) at a wavelength of 570 nm. For temozolomide (TMZ)-induced cellular toxicity, cells were treated with 100 μM of TMZ (Selleck, cat. no. S1237) for 24 h and apoptosis was detected using western blotting.

Colony formation assay. U-87MG/NC, U-87MG/sh-TIGAR cells, U-87MG/pcDNA3.1 and U-87MG/pcDNA3.1-TIGAR cells (200 cells/well) were plated into a 6-well plate and cultured for 14 days at 37˚C. The media were then removed, and cells were fixed with 4% paraformaldehyde at room temperature for 10 min and stained with 1% crystal violet in 2% ethanol at room temperature for 20 min. Visible colonies were counted by eye.

Western blotting assay. Total protein was extracted from whole cell lysates using RIPA buffer, and the protein concentration was measured using a bicinchoninic acid assay. The protein samples (30 μg/lane) were separated by 12.5% SDS-PAGE. Proteins were transferred to polyvinylidene difluoride membranes (EMD Millipore) at 300 mA for 90 min. Subsequently, the membranes were blocked at room temperature for 1 h with Tris-buffered saline containing 0.1% Tween-20 (TBST) and 5% dry milk and incubated overnight with primary antibodies at 4˚C. Membranes were washed three times with TBST and incubated for 2 h with secondary antibodies at room temperature. After washing for three times with TBST, blots were detected using enhanced chemiluminescence (ECL) reagents (Thermo Fisher Scientific, Inc) and captured by a Luminescent Image Analyzer LAS-3000 (Fujifilm Holdings Corporation), and the optical densities of antibody-specific bands were analyzed using ImageJ version 1.37 (National Institutes of Health).

Co-immunoprecipitation (Co-IP). Cells were harvested by centrifugation at 500 x g for 5 min at 4˚C and lysed in RIPA lysis buffer for 30 min. Following centrifugation at 13,000 x g for 15 min 4˚C, the 1/10 volume of supernatant was collected as input, the 1/2 volume of remaining supernatant was
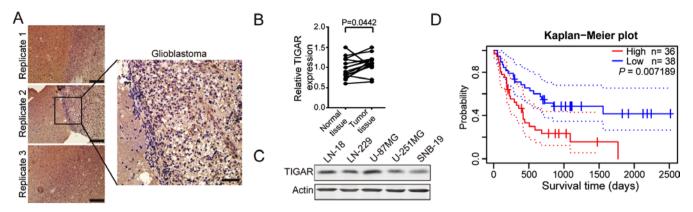
Figure 1. TIGAR is overexpressed in glioblastoma tissues and is associated with poor survival. (A) Immunohistochemical staining of TIGAR indicated that, compared with adjacent normal tissues, TIGAR was overexpressed in glioblastoma tissues. Scale bar, 200 μm in replicate images and 50 μm in enlarged image. (B) Quantitative analysis of TIGAR staining between normal and tumor tissues (n=15). (C) Protein lysates prepared from five human glioblastoma cell lines were immunoblotted with anti-TIGAR antibody, and TIGAR was revealed to be overexpressed in U-87MG cells. (D) Kaplan-Meier analysis of overall survival in patients with brain cancer (GSE4412-GPL96) with high or low TIGAR mRNA expression revealed that high expression levels of TIGAR were associated with shorter survival times. These data were obtained from PrognoScan. Data in panel B are expressed as the mean ± standard deviation. TIGAR, TP53 induced glycolysis regulatory phosphatase.

incubated with 1 μg anti-TIGAR (1:200 dilution) or anti-AKT (1:100 dilution) antibody and 40 μl 50% protein A/G agarose slurry at 4°C overnight. The other remaining supernatant was incubated with 1 μg control IgG (1:200 dilution) and 40 μl 50% protein A/G agarose slurry at 4°C overnight. The protein A/G agarose was recovered by centrifugation at 3,000 x g for 5 min at 4°C and washed four times with ice-cold lysis buffer. Proteins were eluted with 2x loading buffer by boiling for 10 min and subjected to immunoblot analysis according to the aforementioned western blotting assay.

ROS, NADPH, glutathione (GSH) and malondialdehyde (MDA) detection. Intracellular ROS were determined using DCFH-DA. A total of 4x10^5 cells were washed with 0.01 M PBS and incubated with 20 μM DCFH-DA at 37°C for 30 min. The cells were visualized using an inverted fluorescence microscope (magnification, x20; Olympus Corporation), and their fluorescence intensity was measured via fluorescence spectrometry (Spectra MaxGemini; Molecular Devices LLC). An NADPH detection kit (cat. no. ECNP-100) was obtained from BioAssay Systems, and GSH (cat. no. S0053) and MDA (cat. no. S0131) were purchased from Beyotime Institute of Biotechnology. The NADPH level, GSH content and MDA level were measured according to the manufacturers' protocols.

Migration and invasion. A Transwell plate (Costar; Corning Inc.) with an 8-μm pore insert was utilized to measure migration and invasion. DMEM containing 10% FBS (0.6 ml) was added to the lower chamber. A total of 5x10^4 U-87MG/nc or U-87MG/sh-TIGAR cells in serum-free DMEM were directly added to the upper chamber and incubated at 37°C for 12 h for the migration assay. To measure invasion, 100 μl diluted Matrigel (1 mg/ml; BD Biosciences) in serum-free cold DMEM was placed in the upper chamber and in the lower chamber, DMEM containing 15% FBS was added, and the cells were incubated at 37°C for 4 h to allow it to set. A total of 5x10^4 U-87MG/nc or U-87MG/sh-TIGAR cells in serum-free DMEM were added directly to the upper chamber

and incubated at 37°C for 24 h. Cells in the lower chamber were fixed with 4% paraformaldehyde at room temperature for 10 min and stained with 1% crystal violet in 2% ethanol at room temperature for 20 min. The numbers of cells in the lower chamber were counted under a light microscope (magnification, x20). At least five fields were analyzed per section.

Immunohistochemistry. Immunohistochemistry was used to detect TIGAR expression levels in surgical resections of glioblastoma tissues collected from 15 male patients (45-55 years old) first diagnosed and admitted to Hunan Cancer Hospital and The Affiliated Cancer Hospital of Xiangya School of Medicine (Changsha, China) between January 2018 and May 2018. The use of glioblastoma samples was approved by the Ethics Committee of Hunan Cancer Hospital and Affiliated Cancer Hospital of Xiangya School of Medicine (no. 20180104). Written informed consent was obtained from all patients prior to enrollment.

The glioblastoma sections were fixed in 4% paraformaldehyde for 2 days at room temperature followed by paraffin-embedding. From the embedded tissue, 5-μm thick sections were cut and deparaffinized in dimethylbenzene, rehydrated in ethanol solutions of 100, 95, and 70% ethanol, and subsequently washed in PBS for 10 min each. Antigen retrieval was performed at 95°C for 20 min, followed by washing with PBS for three times and blocking with 3% BSA for 1 h at room temperature. Sections were incubated with an anti-TIGAR antibody (1:100 dilution) at room temperature for 2 h, and the slides were washed three times with PBS and incubated with components of the GTVisin™ anti-mouse/anti-rabbit immunohistochemical analysis kit, according to the manufacturer's protocols. Glioblastoma tissues and paired normal-appearing tissues in sections were confirmed by Pathology department. Images were captured under a light microscope (magnification, x20). At least five fields were analyzed per section and quantify staining was analyzed using ImageJ version 1.37 (National Institutes of Health)
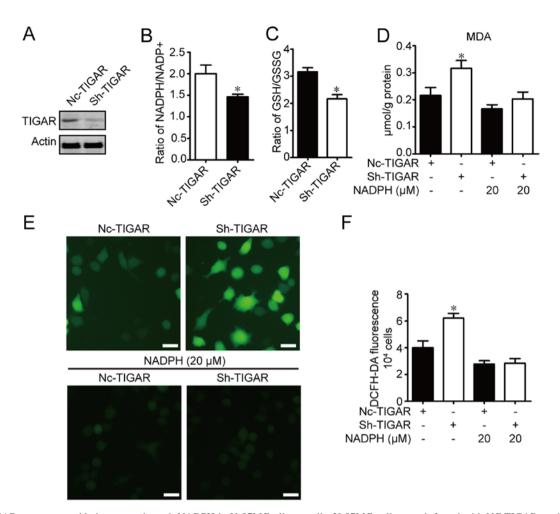
Figure 2. TIGAR attenuates oxidative stress through NADPH in U-87MG glioma cells. U-87MG cells were infected with NC-TIGAR or sh-TIGAR, and were cultured for >2 weeks in the presence of puromycin (2 µg/ml) prior to further experiments. (A) TIGAR expression was measured using western blot assay. Ratios of (B) NADPH/NADP$^+$ and (C) GSH/GSSG were measured in U-87MG/NC cells and U-87MG/sh-TIGAR cells. (D) MDA contents were measured in U-87MG/NC, U-87MG/sh-TIGAR, NADPH-pretreated U-87MG/NC and U-87MG/sh-TIGAR cells. (E) Intracellular ROS levels in U-87MG/NC, U-87MG/sh-TIGAR, NADPH-pretreated U-87MG/NC and U-87MG/sh-TIGAR cells were monitored using DCFH-DA under a fluorescence microscope. Scale bar, 20 µm. (F) Intracellular ROS levels in U-87MG/NC, U-87MG/sh-TIGAR, NADPH-pretreated U-87MG/NC and U-87MG/sh-TIGAR cells were determined using DCFH-DA on a microplate reader. The histogram shows the mean ROS production. Data of the triple experiments are presented as the means ± standard deviation. *P<0.05 vs. NC-TIGAR group according to an unpaired t-test/one-way analysis of variance. GSH, glutathione; GSSG, oxidized glutathione; MDA, malondialdehyde; NADP$^+$, nicotinamide adenine dinucleotide phosphate; NADPH, reduced NADP$^+$; NC, negative control shRNA; ROS, reactive oxygen species; sh, short hairpin RNA; TIGAR, TP53 induced glycolysis regulatory phosphatase.

Bioinformatics. Kaplan-Meier survival analysis between TIGAR high expression and low expression in glioma was carried out. Overall survival time based on GSE4412-GPL96 dataset in PrognoScan was performed on PrognoScan (http://dna00.bio.kyutech.ac.jp/PrognoScan/) (11). A total of 74 patients were divided into TIGAR high expression group (n=36) and TIGAR low expression group (n=38) and Cox P-value (P=0.007189) was generated automatically.

Statistical analysis. Experimental data are expressed as the mean ± standard deviation of at least three independent experiments. Statistical analyses were performed using SPSS v18.0 statistical software (SPSS, Inc.). Paired or unpaired Student's t-test were used to compare the significance between two paired groups and two independent groups respectively, and a one-way ANOVA followed by a post-hos Tukey's test was used to determine the significance between three or more independent groups. P<0.05 was considered to indicate a statistically significant difference.

Results

TIGAR is overexpressed in glioblastoma tissues and positively associated with poor prognosis. It has been reported that TIGAR is upregulated in several types of tumor (5-9). To determine whether TIGAR was upregulated in glioblastoma, glioblastoma sections were obtained and subjected to immunohistochemistry. As shown in Fig. 1A and B, TIGAR was significantly overexpressed in glioblastoma tissues compared with paired normal-appearing tissues. TIGAR expression in glioblastoma cell lines, including LN-18, LN-229, U-87MG, U-251MG and SNB-19, was detected. The results revealed that TIGAR was overexpressed in U-87MG cells (Fig. 1C). Furthermore, PrognoScan-based Kaplan-Meier survival analysis (11) revealed an association between elevated TIGAR expression levels and shorter surv]ival duration in the 74 patients with glioblastoma from the database. (Fig. 1D). These results indicated that TIGAR was overexpressed in glioblastoma, and that its expression was negatively associated with survival time.
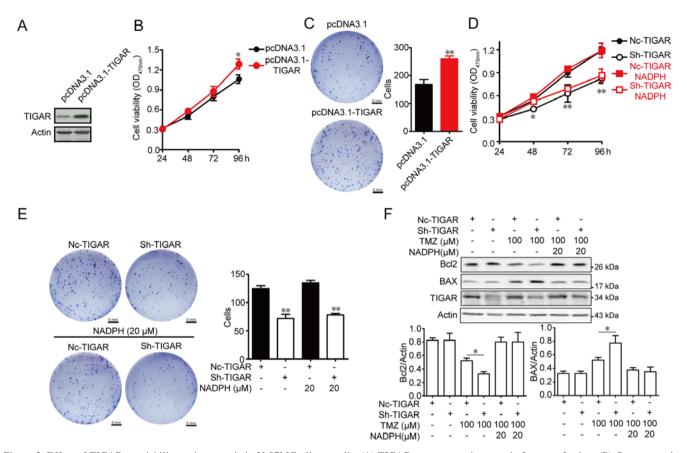
Figure 3. Effect of TIGAR on viability and apoptosis in U-87MG glioma cells. (A) TIGAR content was increased after transfection. (B) Overexpression of TIGAR promoted viability in U-87MG cells, as measured by am MTT assay (n=5). (C) Cells (200) transfected with pcDNA3.1 and pcDNA3.1-TIGAR were seeded into 6-well plates and cultured for 14 days. Colony formation was detected using crystal violet staining. The colony number was counted (n=3). Scale bar, 5 mm. (D) NADPH treatment of TIGAR-knockdown U-87MG cells had no effect on viability (n=5). (E) NADPH treatment of TIGAR-knockdown U-87MG cells had no effect on colony formation (n=3). Scale bar, 5 mm. (F) NADPH (20 μM) addition decreased the expression levels of BAX protein and increased Bcl2 protein expression in 100 μM TMZ-treated TIGAR knockdown U-87MG cells. β-actin was used as an internal control. Bar graphs depict semi-quantitative analysis of Bcl2 and BAX expression (n=3). Data are expressed as the means ± standard deviation. *P<0.05, **P<0.01 vs. pcDNA3.1 or NC-TIGAR. BAX, Bcl2-associated X protein; Bcl2, B cell lymphoma 2; NADPH, reduced nicotinamide adenine dinucleotide phosphate; NC, negative control shRNA; OD, optical density; sh, short hairpin RNA; TIGAR, TP53 induced glycolysis regulatory phosphatase; TMZ, temozolomide.

TIGAR maintains NADPH to alleviate oxidative stress in U-87MG cells. It has been reported that TIGAR promotes NADPH generation through PPP (3). The ratio of NADPH to NADP+ in TIGAR-knockdown U-87MG cells was measured. As shown in Fig. 2A, TIGAR content was decreased in TIGAR-knockdown cells. As shown in Fig. 2B, TIGAR knockdown significantly decreased NADPH content. Glutathione reductase catalyzes the NADPH-driven reduction of oxidized glutathione (GSSG) to GSH (12). Therefore, the ratio of GSH to GSSG was measured in TIGAR-knockdown U-87MG cells. The conversion of GSH from GSSG was significantly reduced in TIGAR-knockdown cells (Fig. 2C). NADPH and GSH are involved in cellular antioxidant responses. Levels of MDA (13), a byproduct of nonenzymatic lipid peroxidation and a principal marker of oxidative stress, were assessed. It has been reported that NADPH addition can protect against DNA damage in TIGAR-knockdown cells (14). Similarly, in the present study, it was observed that TIGAR knockdown significantly increased MDA levels in groups without NADPH treatment, and NADPH inhibited MDA content in TIGAR-knockdown U-87MG cells compared with negative control U-87MG cells although these changes were not significant (Fig. 2D). Additionally, TIGAR knockdown increased intracellular ROS in U-87MG cells

compared with the negative control U-87MG cells, as detected by higher fluorescence following incubation with DCFH-DA. The elevated ROS levels in TIGAR-knockdown U-87MG cells were attenuated by the addition of NADPH (Fig. 2E and F). These results suggested that TIGAR maintained the NADPH level to protect U-87MG cells from oxidative stress.

TIGAR promotes proliferation and inhibits apoptosis in U-87MG cells. To test the effect of TIGAR in glioblastoma, U-87MG cells were transfected with pcDNA3.1-TIGAR, and viability rates were measured. As shown in Fig. 3A-B, TIGAR content was overexpressed after transfection, and TIGAR overexpression significantly increased U-87MG cell viability, and the numbers of cell clones in TIGAR-overexpressing U-87MG cells were higher than in control U-87MG cells (Fig. 3C). The viability of TIGAR-knockdown U-87MG cells was measured, and cell viability was decreased in TIGAR-knockdown U-87MG cells. To ascertain whether the decreased viability of TIGAR knockdown cells was associated with oxidative stress, exogenous NADPH was added. The results revealed that added NADPH did not increase cell viability in TIGAR-knockdown U-87MG cells (Fig. 3D). Additionally, the formation of cell clones was inhibited in TIGAR-knockdown U-87MG cells,
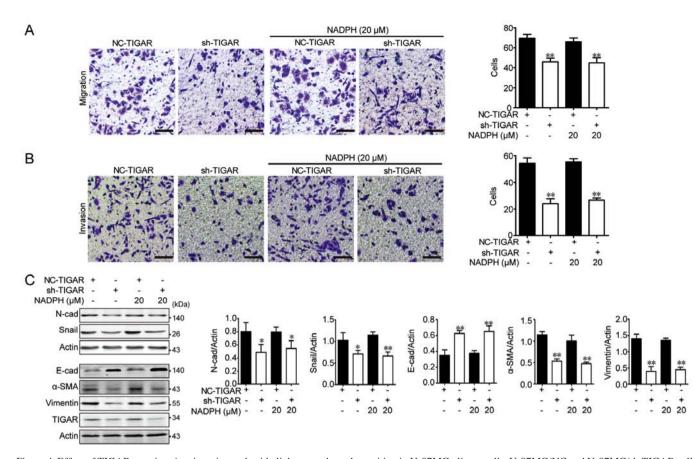
Figure 4. Effect of TIGAR on migration, invasion and epithelial-mesenchymal transition in U-87MG glioma cells. U-87MG/NC and U-87MG/sh-TIGAR cells were stimulated with NADPH for 24 h, and 5x10⁴ cells in serum-free medium were seeded into the upper chamber of Transwell for 12 h. (A) Migration and (B) invasion were decreased in TIGAR-knockdown cells, and NADPH addition had no effect on migration and invasion in TIGAR-knockdown U-87MG cells (n=3). Scale bar, 50 μm. (C) Knockdown of TIGAR increased E-cad, and decreased N-cad, α-SMA, Snail and vimentin protein expression. Added NADPH had no effect on the expression of these proteins. Bar graphs depict semi-quantitative analysis of western blotting for each protein (n=3). *P<0.05, **P<0.01 vs. NC-TIGAR group. Data are presented as the means ± standard deviation. α-SMA, α-smooth muscle actin; E-cad, epithelial cadherin; NADPH, reduced nicotinamide adenine dinucleotide phosphate; N-cad, neural cadherin; NC, negative control; sh, short hairpin RNA; TIGAR, TP53 induced glycolysis regulatory phosphatase.

and additional NADPH did not promote cell growth (Fig. 3E). TMZ-based therapy is the standard of care for patients with glioblastoma, and resistance to TMZ in glioblastoma is a universal phenomenon (15). TIGAR knockdown promoted the TMZ-induced decrease in Bcl2 and increase in BAX protein expression levels, which was indicative of an increase in apoptosis. Furthermore, NADPH significantly alleviated apoptosis in the TMZ-treated U-87MG cells and TIGAR-knockdown U-87MG cells (Fig. 3F). The results indicated that TIGAR promoted viability, and decreased TMZ-induced apoptosis through NADPH-mediated antioxidative activity in U-87MG cells.

TIGAR promotes metastasis in U-87MG cells. Glioblastoma is an aggressive intracranial tumor (16). The number of migratory cells in the Transwell assay was significantly lower in TIGAR-knockdown U-87MG cells, and addition of NADPH did not promote cell migration (Fig. 4A). Additionally, the number of invasive cells was significantly reduced in TIGAR-knockdown U-87MG cells; addition of NADPH failed to promote cell invasion in U-87MG cells (Fig. 4B). The migration and invasion of cancer cells are associated with the epithelial-mesenchymal transition (EMT) (17). Therefore, expression levels of EMT indicators, including N-cadherin,

snail, E-cadherin, α-SMA and vimentin, were assessed. As shown in Fig. 4C, significantly increased E-cadherin, and decreased N-cadherin, α-SMA, snail and vimentin expression levels were observed in TIGAR-knockdown cells, indicating that metastasis was decreased in TIGAR-knockdown U-87MG cells. Notably, the addition of NADPH had no effect on the metastasis of TIGAR-knockdown U-87MG cells, which highlighted the pro-metastatic effect of TIGAR beyond NADPH production in glioblastoma.

TIGAR promotes AKT phosphorylation and interacts with AKT in U-87MG cells. The PI3K/AKT signaling pathway is activated in glioblastoma (18). The activation of AKT promotes cancer growth and metastasis and inhibits autophagy and apoptosis (19). Therefore, PI3K/AKT activation was assessed in TIGAR-knockdown and TIGAR-overexpressing U-87MG cells. As shown in Fig. 5A, no significant differences between total PI3K and p-PI3K levels were identified in TIGAR-knockdown and TIGAR-overexpressing U-87MG cells compared with their respective controls, whereas p-AKT was significantly decreased in TIGAR-knockdown cells and increased in overexpressing cells. To determine whether TIGAR promoted AKT activation in U-87MG cells, TIGAR was transfected into U-87MG cells in a dose-dependent
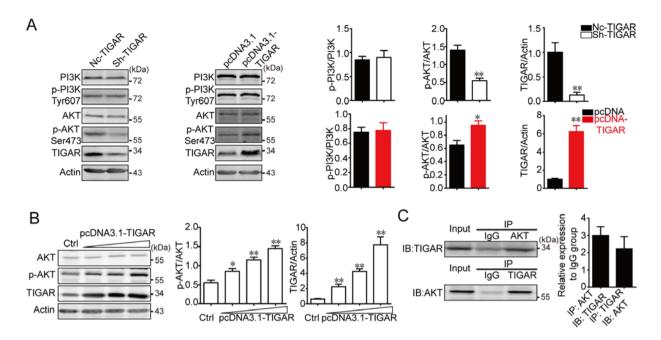
Figure 5. TIGAR promotes AKT activation and interacts with AKT in U-87 glioma cells. (A) U-87MG cells were infected with sh-TIGAR to downregulate TIGAR expression or transfected with pcDNA3.1-TIGAR to increase TIGAR expression. PI3K, p-PI3K, AKT and p-AKT were measured in U-87MG/NC, U-87MG/sh-TIGAR, U-87MG/pcDNA3.1 and U-87MG/pcDNA3.1-TIGAR cells. TIGAR promoted the phosphorylation of AKT. β-actin was used as an internal control. Bar graphs depict semi-quantitative analysis of protein expression levels. (B) U-87MG cells cultured in 6-well plates were transfected with 1, 2 or 3 μg pcDNA3.1-TIGAR. TIGAR promoted the phosphorylation of AKT in a dose dependent manner, which was assessed using western blotting. Bar graphs depict semi-quantitative analysis for p-AKT and TIGAR. (C) Physical interactions between TIGAR and AKT in U-87MG cells were confirmed using a co-immunoprecipitation assay. Bar graph depicts semi-quantitative analysis for TIGAR and AKT when compared with the IgG group. Data of the triple experiments are presented as the means ± standard deviation. $^*P<0.05$, $^{**}P<0.01$ vs. NC-TIGAR or pcDNA3.1. AKT, protein kinase B; Ctrl, control; IgG, immunoglobulin G; NC, negative control; p, phosphorylated; PI3K, phosphoinositide 3-kinase; sh, short hairpin RNA; TIGAR, TP53 induced glycolysis regulatory phosphatase.

manner. The present study demonstrated that p-AKT/AKT markedly increased as TIGAR expression increased (Fig. 5B). Additionally, Co-IP was performed to verify the interaction between TIGAR and AKT. As shown in Fig. 5C, TIGAR interacted with AKT in U-87MG cells. These results indicated that TIGAR promoted AKT activation and interacted with AKT in glioblastoma.

Discussion

Glioma is a type of tumor that occurs in the brain, and 75% of gliomas are astrocytomas (20). Glioblastoma represents the highest grade of astrocytoma, and the overall 5-year survival rate is only 5% (21). Furthermore, glioblastoma is associated with migration, invasion and chemotherapy resistance (22).

TMZ, a second-generation oral alkylating agent that causes DNA damage via methylation of the O(6) position of guanine, is commonly used to treat human malignant glioma. O(6)-methylguanine-DNA methyltransferase mitigates the effectiveness of TMZ and has been used as a marker to predict the efficacy of TMZ treatment (23). In addition, DNA damage response activates p53. However, the high incidence of TP53 mutations leads to p53 loss the function to prevent tumor formation in cancers (24). As a well-known tumor suppressor, the prevailing function of p53 is the transcriptional control of target genes that regulate numerous cellular processes, including the cell cycle, apoptosis, autophagy and metabolism (25). TMZ treatment induces p53 activation and subsequent upregulation of p21, Noxa and BAX (26).

As a downstream target protein of p53, TIGAR expression is dependent on p53, whereas p73, p63, hypoxia inducible factor 1 and Sp1 transcription factor also promote TIGAR expression (27,28). A number of studies have demonstrated that chemotherapy is accompanied by increased TIGAR expression, and TIGAR-derived NADPH protects cancer cells from chemotherapy-induced damage (29,30). Additionally, nuclear localized TIGAR exhibits antioxidant properties, and provides ribose-5-phosphate for DNA repair following epirubicin treatment (31). TIGAR is localized in the cytoplasm, endoplasmic reticulum, and the mitochondrial membrane and matrix. In addition to nuclear translocation, TIGAR may translocate to mitochondria under hypoxia in cancer (28). Following cerebral ischemia reperfusion in mice, increased levels of TIGAR are observed in the mitochondrial membrane and matrix, where TIGAR maintains the mitochondrial membrane potential under oxidative stress conditions (32). Therefore, effects of TIGAR beyond oxidation resistance, and the cellular distribution of TIGAR, require further investigation.

The PI3K/AKT signaling pathway serves an important role in the occurrence and development of tumors. This pathway can be activated by various factors, including platelet-derived growth factor, epidermal growth factor and insulin-like growth factor, to promote cell proliferation, differentiation, adhesion and migration, and inhibit apoptosis. Tumor biology studies have mainly concentrated on Class IA PI3K, which is composed of a heterodimer comprising a p110 catalytic subunit and a p85 regulatory subunit (33,34). PI3K binds to the upstream tyrosine receptor kinase via the SH2 region of p85,

causing activation of PI3K. Additionally, PI3K is activated by G protein-coupled receptor (GPCR)-activated Ras upon stimulation with the GPCR ligand cyclic adenosine monophosphate (35). Once PI3K is activated, its activated substrates phosphatidylinositol (PI) 4,5-bisphosphate (PI(4,5)P$_2$) and PI (3,4,5)-trisphosphate (PIP$_3$) act as second messengers to activate and form a signaling cascade complex, leading to the phosphorylation of AKT.

PI3K phosphorylates AKT at Thr308 and Ser473 to activate AKT. PI3K catalyzes the phosphorylation of PI 4-phosphate and PI(4,5)P$_2$ at their third positions, and converts them into PI(3,4)P$_2$ and PIP$_3$ to recruit AKT (36). AKT can be directly activated by PI(3,4)P$_2$. However, PIP$_3$ activates phosphoinositide-dependent kinase (PDK)-1 to phosphorylate AKT at Thr308, and AKT is further phosphorylated at Ser473 and fully activated in the presence of PDK-2. The tumor suppressor PTEN reverses the transformation of PI(4,5)P$_2$ to PIP$_3$ in the PI3K/AKT pathway, and maintains a low level of PIP$_3$, thereby inhibiting the phosphorylation of AKT. Additionally, it has been confirmed that mammalian target of rapamycin complex 2 (mTORC2) phosphorylates AKT at Ser473, and that this modification requires PIP$_3$ (37).

Activated AKT is involved in the occurrence and development of glioblastoma; the PI3K-AKT-mTOR pathway is frequently activated in glioblastoma to regulate cancer survival (38). Additionally, AKT contributes to glioblastoma formation through the recruitment of existing mRNAs to polysomes (39). The direct and indirect inhibition of AKT activity promotes apoptosis and suppresses glioblastoma growth (40,41).

Due to the small sample size, the association between TIGAR expression and survival time could not be calculated for the patients included in the present study; therefore, the association was analyzed using PrognoScan. As TIGAR is overexpressed in glioblastoma, the role of TIGAR in oxidative stress was investigated. NADPH levels decreased and ROS indicators increased in the TIGAR-knockdown U-87MG glioblastoma cell line. Furthermore, cell viability, TMZ-induced apoptosis, migration, invasion and EMT were investigated in TIGAR-knockdown U-87MG cells. The results demonstrated that TIGAR-mediated antioxidative effects inhibited apoptosis but did not affect viability, migration, invasion or EMT. In addition, TIGAR promoted AKT phosphorylation in a dose-dependent manner and interacted with AKT in U-87MG cells. It has been reported that PFK/FB4, an enzyme similar to TIGAR, phosphorylates nuclear receptor coactivator 3 at Ser857 to enhance its transcriptional activity and promote breast cancer growth and metastasis (42). The manner in which TIGAR, as a phosphatase, promotes AKT phosphorylation requires further investigation.

In conclusion, the results of the present study demonstrated that TIGAR inhibited apoptosis and promoted proliferation, migration and invasion in glioblastoma through NADPH-mediated antioxidative effects and activation of AKT. Therefore, TIGAR may be considered as a potential therapeutic target in glioblastoma.

Acknowledgements

Funding

Availability of data and materials

The datasets used and/or analyzed during the current study are available from the corresponding author on reasonable request.

Authors' contributions

ZT and ZH performed the experiments. ZT analyzed the data. ZH designed the experiments and wrote the manuscript.

Ethics approval and consent to participate

The use of glioblastoma sections was approved by the Ethics Committee of Hunan Cancer Hospital and Affiliated Cancer Hospital of Xiangya School of Medicine (no. 20180104; Changsha, China). All patients provided informed consent.

Patient consent for publication

Not applicable.

Competing interests

The authors declare that they have no competing interests.

References

1. Wen PY and Kesari S: Malignant gliomas in adults. N Engl J Med 359: 492-507, 2008.
2. Stupp R, Taillibert S, Kanner A, Read W, Steinberg D, Lhermitte B, Toms S, Idbaih A, Ahluwalia MS, Fink K, et al: Effect of tumor-treating fields plus maintenance temozolomide vs maintenance temozolomide alone on survival in patients with glioblastoma: A randomized clinical trial. JAMA 318: 2306-2316, 2017.
3. Bensaad K, Tsuruta A, Selak MA, Vidal MN, Nakano K, Bartrons R, Gottlieb E and Vousden KH: TIGAR, a p53-inducible regulator of glycolysis and apoptosis. Cell 126: 107-120, 2006.
4. Green DR and Chipuk JE: P53 and metabolism: Inside the TIGAR. Cell 126: 30-32, 2006.
5. Agnoletto C, Melloni E, Casciano F, Rigolin GM, Rimondi E, Celeghini C, Brunelli L, Cuneo A, Secchiero P and Zauli G: Sodium dichloroacetate exhibits anti-leukemic activity in B-chronic lymphocytic leukemia (B-CLL) and synergizes with the p53 activator Nutlin-3. Oncotarget 5: 4347-4360, 2014.
6. Zhou X, Xie W, Li Q, Zhang Y, Zhang J, Zhao X, Liu J and Huang G: TIGAR is correlated with maximal standardized uptake value on FDG-PET and survival in non-small cell lung cancer. PLoS One 8: e80576, 2013.
7. Ko YH, Domingo-Vidal M, Roche M, Lin Z, Whitaker-Menezes D, Seifert E, Capparelli C, Tuluc M, Birbe RC, Tassone P, et al: TIGAR metabolically reprograms carcinoma and stromal cells in breast cancer. J Biol Chem 116: 740209, 2016.
8. Zou S, Gu Z, Ni P, Liu X, Wang J and Fan Q: SP1 plays a pivotal role for basal activity of TIGAR promoter in liver cancer cell lines. Mol Cell Biochem 359: 17-23, 2012.
9. Cheung EC, Athineos D, Lee P, Ridgway RA, Lambie W, Nixon C, Strathdee D, Blyth K, Sansom OJ and Vousden KH: TIGAR is required for efficient intestinal regeneration and tumorigenesis. Dev Cell 25: 463-477, 2013.
10. Lee P, Vousden KH and Cheung EC: TIGAR, TIGAR, burning bright. Cancer Metab 2: 1, 2014.
11. Mizuno H, Kitada K, Nakai K and Sarai A: PrognoScan: A new database for meta-analysis of the prognostic value of genes. BMC Med Genomics 2: 18, 2009.

12. Griffith OW: Determination of glutathione and glutathione disulfide using glutathione reductase and 2-vinylpyridine. Anal Biochem 106: 207-212, 1980.
13. Nielsen F, Mikkelsen BB, Nielsen JB, Andersen HR and Grandjean P.: Plasma malondialdehyde as biomarker for oxidative stress: Reference interval and effects of life-style factors. Clin Chem 43: 1209-1214, 1997.
14. Xie JM, Li B, Yu HP, Gao QG, Li W, Wu HR and Qin ZH: TIGAR has a dual role in cancer cell survival through regulating apoptosis and autophagy. Cancer Res 74: 5127-5138, 2014.
15. Lee SY: Temozolomide resistance in glioblastoma multiforme. Genes Dis 3: 198-210, 2016.
16. Zeng WF, Navaratne K, Prayson RA and Weil RJ: Aurora B expression correlates with aggressive behaviour in glioblastoma multiforme. J Clin Pathol 60: 218-221, 2007.
17. Heerboth S, Housman G, Leary M, Longacre M, Byler S, Lapinska K, Willbanks A and Sarkar S: EMT and tumor metastasis. Clin Transl Med 4: 6, 2015.
18. Li X, Chen N, Gu H, Yen A, Cao L, Wang E and Wang L: PI3K/Akt/mTOR signaling pathway and targeted therapy for glioblastoma. Oncotarget 7: 33440-33450, 2016.
19. Agarwal E, Brattain MG and Chowdhury S: Cell survival and metastasis regulation by Akt signaling in colorectal cancer. Cell Signal 25: 1711-1719, 2013.
20. Gladson CL, Prayson RA and Liu WM: The pathobiology of glioma tumors. Annu Rev Pathol 5: 33-50, 2010.
21. Delgado-Lopez PD and Corrales-Garcia EM: Survival in glioblastoma: A review on the impact of treatment modalities. Clin Transl Oncol 18: 1062-1071, 2016.
22. Xie Q, Mittal S and Berens ME: Targeting adaptive glioblastoma: An overview of proliferation and invasion. Neuro Oncol 16: 1575-1584, 2014.
23. Chen X, Zhang M, Gan H, Wang H, Lee JH, Fang D, Kitange GJ, He L, Hu Z, Parney IF, et al: A novel enhancer regulates MGMT expression and promotes temozolomide resistance in glioblastoma. Nat Commun 9: 2949, 2018.
24. Blagosklonny MV: Loss of function and p53 protein stabilization. Oncogene 15: 1889-1893, 1997.
25. Fischer M: Census and evaluation of p53 target genes. Oncogene 36: 3943-3956, 2017.
26. Zhang WB, Wang Z, Shu F, Jin YH, Liu HY, Wang QJ and Yang Y: Activation of AMP-activated protein kinase by temozolomide contributes to apoptosis in glioblastoma cells via p53 activation and mTORC1 inhibition. J Biol Chem 285: 40461-40471, 2010.
27. Lee P, Hock A, Vousden K and Cheung E: P53-and p73-independent activation of TIGAR expression in vivo. Cell Death Dis 6: e1842, 2015.
28. Cheung EC, Ludwig RL and Vousden KH: Mitochondrial localization of TIGAR under hypoxia stimulates HK2 and lowers ROS and cell death. Proc Natl Acad Sci USA 109: 20491-20496, 2012.
29. Zhang Y, Chen F, Tai G, Wang J, Shang J, Zhang B, Wang P, Huang B, Du J, Yu J, et al: TIGAR knockdown radiosensitizes TrxR1-overexpressing glioma in vitro and in vivo via inhibiting Trx1 nuclear transport. Sci Rep 7: 42928, 2017.
30. Zhang H, Gu C, Yu J, Wang Z, Yuan X, Yang L, Wang J, Jia Y, Liu J and Liu F: Radiosensitization of glioma cells by TP53-induced glycolysis and apoptosis regulator knockdown is dependent on thioredoxin-1 nuclear translocation. Free Radic Biol Med 69: 239-248, 2014.
31. Yu HP, Xie JM, Li B, Sun YH, Gao QG, Ding ZH, Wu HR and Qin ZH: TIGAR regulates DNA damage and repair through pentosephosphate pathway and Cdk5-ATM pathway. Sci Rep 5: 9853, 2015.
32. Li M, Sun M, Cao L, Gu JH, Ge J, Chen J, Han R, Qin YY, Zhou ZP, Ding Y and Qin ZH: A TIGAR-regulated metabolic pathway is critical for protection of brain ischemia. J Neurosci 34: 7458-7471, 2014.
33. Oda K, Stokoe D, Taketani Y and McCormick F: High frequency of coexistent mutations of PIK3CA and PTEN genes in endometrial carcinoma. Cancer Res 65: 10669-10673, 2005.
34. Luo J, Manning BD and Cantley LC: Targeting the PI3K-Akt pathway in human cancer: Rationale and promise. Cancer Cell 4: 257-262, 2003.
35. Vanhaesebroeck B, Guillermet-Guibert J, Graupera M and Bilanges B: The emerging mechanisms of isoform-specific PI3K signalling. Nat Rev Mol Cell Biol 11: 329-341, 2010.
36. Zhao L and Vogt PK: Class I PI3K in oncogenic cellular transformation. Oncogene 27: 5486-5496, 2008.
37. Ebner M, Sinkovics B, Szczygiel M, Ribeiro DW and Yudushkin I: Localization of mTORC2 activity inside cells. J Cell Biol 216: 343-353, 2017.
38. Fan QW and Weiss WA: Autophagy and Akt promote survival in glioma. Autophagy 7: 536-538, 2011.
39. Rajasekhar VK, Viale A, Socci ND, Wiedmann M, Hu X and Holland EC: Oncogenic Ras and Akt signaling contribute to glioblastoma formation by differential recruitment of existing mRNAs to polysomes. Mol Cell 12: 889-901, 2003.
40. Gao T, Furnari F and Newton AC: PHLPP: A phosphatase that directly dephosphorylates Akt, promotes apoptosis, and suppresses tumor growth. Mol Cell 18: 13-24, 2005.
41. Assad Kahn S, Costa SL, Gholamin S, Nitta RT. Dubois LG, Fève M, Zeniou M, Coelho PL, El-Habr E, Cadusseau J, et al: The anti-hypertensive drug prazosin inhibits glioblastoma growth via the PKCdelta-dependent inhibition of the AKT pathway. EMBO Mol Med 8: 511-526, 2016.
42. Dasgupta S, Rajapakshe K, Zhu B, Nikolai BC, Yi P, Putluri N, Choi JM, Jung SY, Coarfa C, Westbrook TF, et al: Metabolic enzyme PFKFB4 activates transcriptional coactivator SRC-3 to drive breast cancer. Nature 556: 249-254, 2018.